Influence of the interaction between phonons on the properties of the surface magnetopolaron in polar crystals

Jing-Lin Xiao and Wei Xiao

*Chinese Centre of Advanced Science and Technology (World Laboratory), P.O. Box 8730, Beijing 100080, People's Republic of China; Laboratory of Excited State Processes, Changchun Institute of Physics Academia Sinica, Changchun 130021, People's Republic of China; and Department of Physics, Inner Mongolia National Teacher's College, Tongliao 028043, People's Republic of China**

(Received 24 July 1996; revised manuscript received 12 May 1997)

There is weak bulk but strong surface coupling between the electron and phonons for polar crystals in a magnetic field. In this paper, the influences of the electron interaction with both the weak-coupling bulk longitudinal-optical phonons and the strong-coupling surface-optical phonons on the properties of the surface polaron in a magnetic field are studied. If we consider the interaction between phonons of different wave vectors in the recoil process, the magnetic-field dependence of the cyclotron-resonance frequency, induced potential, the effective interaction potential, and the cyclotron-resonance mass of the surface magnetopolaron is obtained by using a linear-combination operator and perturbation method. Numerical calculations, for the AgCl crystal as an example, are performed and some properties of these quantities of the surface polaron in a magnetic field are discussed. [S0163-1829(98)06508-4]

I. INTRODUCTION

With the development of magneto-optical technology, the properties of the polaron for polar crystals in magnetic field of arbitrary strength have been of considerable interest.[1–4] In the early 1970s, Evans and Mills,[5,6] using a variational approach, investigated the case where the electron interacted with both surface and bulk longitudinal-optical waves and the phonons were considered as the only electric-dipole active excitations. Larsen[7] proposed a fourth-order perturbation method to investigate the properties of two-dimensional polarons. Considering both the electron-bulk–longitudinal-optical (LO) phonon and electron-surface-optical (SO)–phonon interaction, Kong, Wei, and Gu[8] have generalized this method to treat the magnetopolaron in a semiconductor quantum well. Later, Osorio, Maialle, and Hipolito[9] reported for the time a theoretical calculation for the resonant donor-impurity magnetopolaron in GaAs-$Ga_{1-x}Al_xAs$ quantum-well structures. Employing Haga's perturbation method, Hu *et al.*[10] derived an effective Hamiltonian for the interface magnetopolaron in polar crystals at zero temperature, in which the interactions of both bulk LO phonons and interface phonons have been taken into account. Wei and co-workers[11,12] studied the induced potential and the self-energy of an interface magnetopolaron interacting with bulk LO phonons as well as interface optical phonons using the Green-function method.

Huybrechts[13] proposed a linear combination operator method, by which a strong-coupling polaron was investigated. Later, other authors[14,15] studied the strong-coupling polaron in many aspects by this method. On the basis of Huybrechts's work, Tokuda[16] added another variational parameter to the momentum operator and also evaluated the ground-state energy and effective mass of the bulk polaron.

For the bulk polaron, the weak- and intermediate-coupling theories are applicable for the electron-bulk–LO-phonon coupling constant $\alpha<6$,[17] whereas for the surface polaron, this confinement is about 2.5.[18] There is weak coupling between the electron and the bulk LO phonon but strong coupling between the electron and the SO phonon for many polar crystals. So far, research into this has been very scarce. The properties of the surface or interface polaron in corresponding polar crystals have been discussed by the method of a linear-combination operator and a simple unitary transformation by the present authors.[19,20]

The ground-state energy and the cyclotron-resonance mass of the surface polaron in magnetic field has been calculated by many methods. Many of them mainly concentrated their attention on the weak- and intermediate-coupling cases. However, the surface magnetopolaron in strong-coupling polar crystals has not been investigated so far. In fact, so far research of the polaron only was restricted to the approximation and calculation where the interaction between phonons of different wave vectors in the recoil process is neglected. The properties of the surface polaron, which considers the corresponding interaction, have been discussed by the perturbation method by the present authors and co-workers.[21]

The purpose of this present paper is to explore the effect of the interaction between phonons of different wave vectors in the recoil process on the properties of the surface polaron in magnetic field. With both the weak coupling between the electron and bulk LO phonon and the strong coupling between the electron and SO phonon included, we obtain an expression for the effective Hamiltonian of the surface polaron in magnetic field. If we consider the interaction between phonons of different wave vectors in the recoil process, the influence on the effective Hamiltonian, induced potential, effective interaction potential, and effective mass of the surface magnetopolaron are investigated. Numerical calculations, taking AgCl crystal as an example, are performed and the properties of these quantities for the surface magnetopolaron in polar crystals are discussed.

0163-1829/98/58(3)/1678(11)/$15.00 PRB 58

II. HAMILTONIAN

Now we discuss a surface magnetopolaron in polar crystal AgCl and vacuum. There are polar crystal AgCl and vacuum in the $z>0$ and $z<0$ semispaces, respectively. The x-y plane is their interface. The static uniform magnetic field is along the z direction $\mathbf{B}=(0,0,B)$ and described by a vector potential in the Landau gauge $\mathbf{A}=B(-y/2,x/2,0)$. An electron moves in polar crystals AgCl, i.e., the $z>0$ side, so there is a barrier from vacuum to it. We suppose that the barrier is infinitely high; therefore, the electron is restricted within AgCl crystal at a distance z (>0) from the surface. The Hamiltonian of the electron, interacting with both the bulk LO phonon and SO phonon can be written as ($\hbar=m=1$; m is the band mass of the electron)

$$H=\frac{1}{2}\left(P_x-\frac{\beta^2}{4}y\right)^2+\frac{1}{2}\left(P_y+\frac{\beta^2}{4}x\right)^2+\frac{P_z^2}{2}$$
$$+\frac{e^2(\varepsilon_\infty-1)}{4Z\varepsilon_\infty(\varepsilon_\infty+1)}+\sum_{\mathbf{W}}\omega_l a_{\mathbf{W}}^\dagger a_{\mathbf{W}}+\sum_{\mathbf{Q}}\omega_S b_{\mathbf{Q}}^\dagger b_{\mathbf{Q}}$$
$$+\sum_{\mathbf{W}}\frac{1}{W}\sin(W_z z)(V_W^* e^{-i\mathbf{W}_\parallel\cdot\boldsymbol{\rho}}a_W^\dagger+\text{H.c.})$$
$$+\sum_{\mathbf{Q}}\frac{1}{\sqrt{Q}}e^{-QZ}(c^* e^{-i\mathbf{Q}\cdot\boldsymbol{\rho}}b_{\mathbf{Q}}^\dagger+\text{H.c.}), \tag{1a}$$

$$V_W^*=i\left(\frac{4\pi e^2\omega_l}{\varepsilon V}\right)^{1/2}, \tag{1b}$$

$$c^*=i\left(\frac{\pi e^2\omega_s}{\varepsilon^* S}\right)^{1/2}, \tag{1c}$$

$$\frac{1}{\varepsilon}=\frac{1}{\varepsilon_\infty}-\frac{1}{\varepsilon_0}, \tag{1d}$$

$$\frac{1}{\varepsilon^*}=\frac{\varepsilon_0-1}{\varepsilon_0+1}-\frac{\varepsilon_\infty-1}{\varepsilon_\infty+1}, \tag{1e}$$

$$\omega_S^2=\tfrac{1}{2}(\omega_T^2+\omega_l^2), \tag{1f}$$

$$\beta^2=\frac{2e}{c}B. \tag{1g}$$

Here the electron has position vector (x,y,z) with $\boldsymbol{\rho}=(x,y,0)$ and momentum $\mathbf{P}=(P_x,P_y,P_z)$. $a_{\mathbf{w}}^\dagger$ and $a_{\mathbf{w}}$ are the creation and annihilation operators, respectively, of a bulk LO phonon with a three-dimensional wave vector $\mathbf{W}=(W_x,W_y,W_z)$ with frequency ω_l and projection $W_\parallel=(W_x,W_y,0)$. $b_{\mathbf{Q}}^\dagger$ and $b_{\mathbf{Q}}$ are the corresponding operators for the SO phonon with a two-dimensional wave vector $\mathbf{Q}$ with frequency ω_S. ω_T is the frequency of bulk transverse-optical phonon. S and V are the surface area and the volume, respectively, of the AgCl crystal. ε_0 (ε_∞) is the static (high-frequency) dielectric constant.

The Hamiltonian can formally be divided into two parts

$$H=H_\parallel+H_z, \tag{2a}$$

$$H_z=\frac{P_z^2}{2}+\frac{e^2(\varepsilon_\infty-1)}{4Z\varepsilon_\infty(\varepsilon_\infty+1)}, \tag{2b}$$

and the rest is called $H_\parallel$. On the assumption that the motion in the z direction is slow, in determining the motion state in the x-y plane, quantities such as the momentum and position in the z direction may be regarded as parameters. This procedure is exactly analogous to the quasiadiabatic approximation.[22]

For motion parallel to the x-y plane, we introduce the unitary transformation

$$U_1=\exp\left(-iA_1\sum_{\mathbf{W}}a_{\mathbf{W}}^\dagger a_{\mathbf{W}}\mathbf{W}_\parallel\cdot\boldsymbol{\rho}-iA_2\sum_{\mathbf{Q}}b_{\mathbf{Q}}^\dagger b_{\mathbf{Q}}\mathbf{Q}\cdot\boldsymbol{\rho}\right), \tag{3a}$$

where A_i ($i=1,2$) is a parameter characterizing the coupling strength. In the unitary transformation U_1, where $A_1=1$ corresponds to the weak coupling between the electron and bulk LO phonon, and $A_2=0$ corresponds to the strong coupling between the electron and the SO phonon, we can easily obtain

$$U_1=\exp\left(-i\sum_{\mathbf{W}}a_{\mathbf{W}}^\dagger a_{\mathbf{W}}\mathbf{W}_\parallel\cdot\boldsymbol{\rho}\right). \tag{3b}$$

Following Tokuda[16] we also introduce the linear combination of the creation operator $b_j^\dagger$ and annihilation operator b_j to represent the momentum and position of the electron

$$P_{\parallel j}=\left(\frac{\lambda}{2}\right)^{1/2}(b_j+b_j^\dagger+P_{0j}), \tag{3c}$$

$$\rho_j=i\left(\frac{1}{2\lambda}\right)^{1/2}(b_j-b_j^\dagger), \tag{3d}$$

where the subscript j refers to the x and y directions, λ and P_0 are the variational parameters, and $b_j^\dagger$ and b_j are Boson operators satisfying the Boson commutative relation. Carrying out a second unitary transformation,

$$U_2=\exp\left[\sum_{\mathbf{W}}(a_{\mathbf{W}}^\dagger f_W-a_{\mathbf{W}}f_W^*)+\sum_{\mathbf{Q}}(b_{\mathbf{Q}}^\dagger g_Q-b_{\mathbf{Q}}g_Q^*)\right], \tag{3e}$$

where f_W (f_W^*) and g_Q (g_Q^*) are variational parameters. Applying the transformations (3b) and (3e) to the Hamiltonian $H_\parallel$ and using the operator expressions (3c) and (3d) we can easily obtain

$$H=U_2^{-1}U_1^{-1}H_{\parallel}U_1U_2=H_1+H_2, \tag{4a}$$

$$H_1=\frac{\lambda}{4}[(b_x+b_x^\dagger)^2+(b_y+b_y^\dagger)^2]-\frac{\beta^4}{64\lambda}[(b_x-b_x^\dagger)^2+(b_y-b_y^\dagger)^2]+\frac{\lambda}{4}\rho_0^2+\frac{\lambda}{2}\sum_j(b_j+b_j^\dagger)P_{0j}+\sum_{\mathbf{W}}\left(\omega_l+\frac{W_\parallel^2}{2}\right)(a_{\mathbf{W}}^\dagger+f_W^*)$$
$$\times(a_{\mathbf{W}}+f_W)+\sum_{\mathbf{Q}}\omega_s(b_{\mathbf{Q}}^\dagger+g_Q^*)(b_{\mathbf{Q}}+g_Q)+\sum_{\mathbf{W}}\frac{1}{W}\sin(W_zz)[V_W^*(a_{\mathbf{W}}^\dagger+f_W^*)+\text{H.c.}]+\sum_{\mathbf{Q}}\left\{\frac{c^*}{\sqrt{Q}}e^{-QZ}(b_{\mathbf{Q}}^\dagger+g_Q^*)e^{-Q^2/4\lambda}\right.$$
$$\left.\times\exp\left[-\left(\frac{1}{2\lambda}\right)^{1/2}\sum_j Q_jb_j^\dagger\right]\exp\left[\left(\frac{1}{2\lambda}\right)^{1/2}\sum_j Q_jb_j\right]+\text{H.c.}\right\}-\left(\frac{\lambda}{2}\right)^{1/2}\left[(b_x+b_x^\dagger)\sum_{\mathbf{W}}(a_{\mathbf{W}}^\dagger+f_W^*)(a_{\mathbf{W}}+f_W)W_x+(b_y+b_y^\dagger)\right.$$
$$\left.\times\sum_{\mathbf{W}}(a_{\mathbf{W}}^\dagger+f_W^*)(a_{\mathbf{W}}+f_W)W_y\right]-i\frac{\beta^2}{8}[(b_x+b_x^\dagger)(b_y-b_y^\dagger)-(b_y+b_y^\dagger)(b_x-b_x^\dagger)]+i\frac{\beta^2}{4}\left(\frac{1}{2\lambda}\right)^{1/2}\left[(b_y-b_y^\dagger)\sum_{\mathbf{W}}(a_{\mathbf{W}}^\dagger+f_W^*)\right.$$
$$\left.\times(a_{\mathbf{W}}+f_W)W_x-(b_x-b_x^\dagger)\sum_{\mathbf{W}}(a_{\mathbf{W}}^\dagger+f_W^*)(a_{\mathbf{W}}+f_W)W_y\right]+i\frac{\beta^2}{8}[(b_x-b_x^\dagger)P_{0y}-(b_y-b_y^\dagger)P_{0x}]-\left(\frac{\lambda}{2}\right)^{1/2}$$
$$\times\sum_{\mathbf{W}}(a_{\mathbf{W}}^\dagger+f_W^*)(a_{\mathbf{W}}+f_W)(W_xP_{0x}+W_yP_{0y}), \tag{4b}$$

$$H_2=\tfrac{1}{2}\sum_{\mathbf{W}\neq\mathbf{W}'}(a_{\mathbf{W}}^\dagger+f_W^*)(a_{\mathbf{W}}+f_W)(a_{\mathbf{W}'}^\dagger+f_{W'}^*)(a_{\mathbf{W}'}+f_{W'})(W_xW_x'+W_yW_y'). \tag{4c}$$

The ground-state wave function of the system is $|\phi\rangle=|\varphi(\rho)\rangle|0\rangle|0\rangle_b$ where $|\varphi(\rho)\rangle$ is the normalized surface magnetopolaron wave function. $|0\rangle$ is the zero-phonon state and $|0\rangle_b$ is the vacuum state of the b operator, which satisfied

$$a_{\mathbf{W}}|0\rangle=b_{\mathbf{Q}}|0\rangle=0,\quad b_j|0\rangle_b=0. \tag{5}$$

In the variation for minimizing the ground-state energy with respect to the variational parameters, the total momentum parallel to the x-y plane can be written as

$$\mathbf{P}_{\parallel T}=\mathbf{P}_\parallel+\sum_{\mathbf{W}}a_{\mathbf{W}}^\dagger a_{\mathbf{W}}\mathbf{W}_\parallel+\sum_{\mathbf{Q}}b_{\mathbf{Q}}^\dagger b_{\mathbf{Q}}\mathbf{Q}. \tag{6}$$

According to the Tokuda[16] method, the minimization problem is now carried out by the use of the Lagrange multipliers. Choosing an arbitrary constant multiplier u, we have

$$\langle\phi|H_1-U_2^{-1}U_1^{-1}\mathbf{u}\cdot\mathbf{P}_{\parallel T}U_1U_2|\phi\rangle=\langle\varphi(\rho)|F(\lambda,f_W,g_Q,u,P_0)|\varphi(\rho)\rangle, \tag{7a}$$

$$F(\lambda,f_W,g_Q,u,P_0)={}_b\langle0|\langle0|H_1-U_2^{-1}U_1^{-1}\mathbf{u}\cdot\mathbf{P}_{\parallel T}U_1U_2|0\rangle|0\rangle_b=\frac{\lambda}{2}+\frac{\lambda}{4}P_0^2+\frac{\beta^4}{32\lambda}+\sum_W\left(\omega_l+\frac{W_\parallel^2}{2}\right)|f_W|^2+\sum_Q\omega_s|g_Q|^2$$
$$+\sum_W\frac{1}{W}\sin(W_zz)(V_W^*f_W^*+\text{H.c.})+\sum_Q\left(\frac{c^*}{\sqrt{Q}}e^{-QZ}g_Q^*e^{-Q^2/4\lambda}+\text{H.c.}\right)-\left(\frac{\lambda}{2}\right)^{1/2}\mathbf{P}_0\cdot\mathbf{u}-\sum_Q\mathbf{Q}\cdot\mathbf{u}|g_Q|^2$$
$$-\left(\frac{\lambda}{2}\right)^{1/2}\sum_W\mathbf{W}_\parallel\cdot\mathbf{P}_0|f_W|^2. \tag{7b}$$

$F(\lambda, f_W, g_Q, u, P_0)$ may be called the variational parameters function. Minimizing Eq. (7b) with respect to λ, f_W, g_Q, u, and P_0, we can determine these parameters. Using the variational method, we get

$$f_W = -\frac{V_W^* \sin(W_z z)}{W\left[\omega_l + \frac{W_\parallel^2}{2} - \left(\frac{\lambda}{2}\right)^{1/2} \mathbf{W}_\parallel \cdot \mathbf{P}_0\right]}, \tag{8a}$$

$$g_Q = -\frac{c^* e^{-QZ} e^{-Q^2/4\lambda}}{\sqrt{Q}(\omega_s - \mathbf{Q}\cdot\mathbf{u})}. \tag{8b}$$

Substituting Eq. (8) into Eq. (7b), we have

$$F(\lambda,u,P_0) = \frac{\lambda}{2} + \frac{\lambda}{4} P_0^2 + \frac{\omega_c^2}{8\lambda} - \left(\frac{\lambda}{2}\right)^{1/2} \mathbf{P}_0\cdot\mathbf{u} - \sum_W \frac{|V_W|^2 \sin^2(W_z z)}{W^2\left[\omega_l + \frac{W_\parallel^2}{2} - \left(\frac{\lambda}{2}\right)^{1/2} \mathbf{W}_\parallel\cdot\mathbf{P}_0\right]} - \sum_Q \frac{|c|^2 e^{-2QZ} e^{-Q^2/2\lambda}}{Q(\omega_s - \mathbf{Q}\cdot\mathbf{u})}, \tag{9a}$$

$$\omega_c = \frac{e\beta}{c}. \tag{9b}$$

In Eq. (9a), the last two terms can be represented as

$$-\sum_W \frac{|V_W|^2 \sin^2(W_z z)}{W^2\left[\omega_l + \frac{W_\parallel^2}{2} - \left(\frac{\lambda}{2}\right)^{1/2} \mathbf{W}_\parallel\cdot\mathbf{P}_0\right]} - \sum_Q \frac{|c|^2 e^{-2QZ} e^{-Q^2/2\lambda}}{Q(\omega_s - \mathbf{Q}\cdot\mathbf{u})}$$
$$= -\sum_W \frac{|V_W|^2 \sin^2(W_z z)}{W^2\left(\omega_l + \frac{W_\parallel^2}{2}\right)} \left(1 + \frac{\frac{\lambda}{2}(\mathbf{W}_\parallel\cdot\mathbf{P}_0)^2}{\left(\omega_l + \frac{W_\parallel^2}{2}\right)^2} + \cdots\right) - \sum_Q \frac{|c|^2 e^{-2QZ}}{Q\omega_s}\left(1 + \frac{(\mathbf{Q}\cdot\mathbf{u})^2}{\omega_s^2} + \cdots\right) e^{-Q^2/2\lambda}. \tag{9c}$$

Equation (9c), it can be calculated by replacing the summation with integration and expanding them up to the second-order term of u and P_0 for a slow electron.[16] In this expression, the first-order terms in $\mathbf{P}_0\cdot\mathbf{W}_\parallel$ and $\mathbf{Q}\cdot\mathbf{u}$ are equal to zero; we have

$$F(\lambda,u,P_0) = \frac{\lambda}{2} + \frac{\lambda}{4} P_0^2 + \frac{\omega_c^2}{8\lambda} - \left(\frac{\lambda}{2}\right)^{1/2} \mathbf{P}_0\cdot\mathbf{u} - \alpha_l\omega_l\left[\frac{\pi}{2} - K(Z)\right] - \frac{\lambda}{2}\alpha_l P_0^2\left(\frac{\pi}{16} - L(Z)\right) - \frac{\sqrt{\pi}}{2}\alpha_S\omega_s\left(\frac{\lambda}{\omega_l}\right)^{1/2}$$
$$\times e^{(\lambda/\omega_l)u_l^2 Z^2} \operatorname{erfc}\left[\left(\frac{\lambda}{\omega_l}\right)^{1/2} u_l Z\right] - \alpha_s\left(\frac{\lambda}{\omega_s}\right)^{3/2} u^2 M(Z), \tag{10a}$$

$$K(Z) = \int_0^\infty \frac{e^{-2u_l z x}}{1+x^2}\, dx, \tag{10b}$$

$$L(Z) = \int_0^\infty \frac{x^2 e^{-2u_l z x}}{(1+x^2)^3}\, dx, \tag{10c}$$

$$M(z) = \int_0^\infty x^2 e^{-x^2 - 2u_\lambda z x} dx, \tag{10d}$$

$$\alpha_l = \frac{e^2}{\varepsilon u_l}, \quad \alpha_s = \frac{e^2}{\varepsilon^* u_s}, \quad u_l = (2\omega_l)^{1/2}, \tag{10e}$$

$$u_s = (2\omega_s)^{1/2}, \quad u_\lambda = (2\lambda)^{1/2}, \quad x = \frac{W_\parallel}{u_l}. \tag{10f}$$

The extremum condition $\alpha F/\alpha P_0 = 0$ gives

$$\mathbf{P}_0 = \frac{(2/\lambda)^{1/2}}{1 - \frac{\pi}{8}\alpha_l + 2\alpha_l L(z)}\, \mathbf{u}. \tag{11}$$

Substituting Eq. (11) into Eq. (10a), we get

$$F(\lambda,u)=\frac{\lambda}{2}+\frac{\omega_c^2}{8\lambda}-\alpha_l\omega_l\left(\frac{\pi}{2}-K(Z)\right)-\frac{\sqrt{\pi}}{2}\alpha_s\omega_s\left(\frac{\lambda}{\omega_s}\right)^{1/2}e^{-(\lambda/\omega_l)u_l^2z^2}\operatorname{erfc}\left[\left(\frac{\lambda}{\omega_l}\right)^{1/2}u_lZ\right]-\frac{1}{2}u^2$$
$$\times\left[\frac{1}{1-\frac{\pi}{8}\alpha_l+2\alpha_lL(Z)}+2\alpha_s\left(\frac{\lambda}{\omega_s}\right)^{3/2}M(Z)\right]. \quad (12)$$

For a slow electron, u is very small; one can omit the final term in Eq. (12) so that the variation in $F(\lambda,u)$ with respect to λ yields

$$\lambda=\left[\frac{\omega_c^2}{4}+\frac{\sqrt{\pi}}{2}\alpha_s\sqrt{\omega_s}\lambda^{3/2}e^{(\lambda/\omega_l)u_l^2z^2}\operatorname{erfc}\left[\left(\frac{\lambda}{\omega_l}\right)^{1/2}u_lz\right]-2\alpha_su_lz\left(\frac{\omega_s}{\omega_l}\right)^{1/2}\lambda^2\int_0^\infty xe^{-x^2-2(\lambda/\omega_l)^{1/2}u_lzx}dx\right]^{1/2}. \quad (13)$$

For the momentum expectation value of the surface magnetopolaron we find

$$\mathbf{P}={}_b\langle 0|\langle 0|U_2^{-1}U_1^{-1}\mathbf{P}_{\parallel T}U_1U_2|0\rangle|0\rangle_b$$
$$=\left[\frac{1}{1-\frac{\pi}{8}\alpha_l+2\alpha_lL(z)}+2\alpha_s\left(\frac{\lambda}{\omega_s}\right)^{3/2}M(z)\right]\mathbf{u}. \quad (14)$$

It is evident from the structure of this expression that **u** has the meaning of velocity, which may be regarded as the average velocity of the surface magnetopolaron in the x-y plane, and the factor before **u**, namely,

$$m^*=\left[\frac{1}{1-\frac{\pi}{8}\alpha_l+2\alpha_lL(z)}+2\alpha_s\left(\frac{\lambda}{\omega_s}\right)^{3/2}M(z)\right], \quad (15)$$

can be interpreted as the cyclotron-resonance mass of the surface magnetopolaron, which omits the interaction between phonons of different wave vectors in the recoil process. From Eq. (13), one can determine the cyclotron-resonance frequency λ of the surface magnetopolaron at different coordinate z. Finally, the effective Hamiltonian of the surface magnetopolaron in a plane parallel to the surface, which omits the corresponding interaction, can be expressed as

$$\mathcal{H}_{\parallel\,\mathrm{eff}}^0=F(\lambda,u)-{}_b\langle 0|\langle 0|U_2^{-1}U_1^{-1}\mathbf{u}\cdot\mathbf{P}_{\parallel T}U_1U_2|0\rangle|0\rangle_b$$
$$=\frac{\lambda}{2}+\frac{P_\parallel^2}{2m^*}-\alpha_l\omega_l\left(\frac{\pi}{2}-K(Z)\right)+\frac{\omega_c^2}{8\lambda}$$
$$-\frac{\sqrt{\pi}}{2}\alpha_s\omega_s\left(\frac{\lambda}{\omega_s}\right)^{1/2}e^{(\lambda/\omega_l)u_l^2z^2}\operatorname{erfc}\left[\left(\frac{\lambda}{\omega_l}\right)^{1/2}u_lz\right]. \quad (16)$$

III. PERTURBATION CALCULATION

We regard H_1 as the unperturbed Hamiltonian of the surface magnetopolaron-phonon system, and H_2 as the perturbation part in the perturbation calculation. Because the perturbed Hamiltonian H_2 is independent of the operator of the SO phonon $b_{\mathbf{Q}}^\dagger$ ($b_{\mathbf{Q}}$), whereas it is only dependent on the operator of LO phonon $a_{\mathbf{W}}^\dagger$ ($a_{\mathbf{W}}$), the unperturbed eigenstates are denoted by

$$|n\rangle|0\rangle_{b_{\mathbf{Q}}}|0\rangle_b\,, \quad (17a)$$

where n is the number density of bulk LO phonon and $|0\rangle_{b_{\mathbf{Q}}}$ is the zero SO phonon state. The unperturbed ground state is

$$|0\rangle|0\rangle_{b_{\mathbf{Q}}}|0\rangle_b\,. \quad (17b)$$

The unperturbed ground- and excited-state energy are

$$E_0={}_b\langle 0|_{b_{\mathbf{Q}}}\langle 0|\langle 0|H_1|0\rangle|0\rangle_{b_{\mathbf{Q}}}|0\rangle_b$$
$$=\frac{\lambda}{2}+\frac{\beta^4}{32\lambda}+\frac{1}{4}P_0^2+\sum_W\left(\omega_l+\frac{W_\parallel^2}{2}\right)|f_W|^2+\sum_Q\omega_s|g_Q|^2+\sum_W\frac{1}{W}\sin(W_zz)(V_W^*f_W+V_Wf_W^*)$$
$$+\sum_Q\frac{1}{\sqrt{Q}}e^{-QZ}(c^*g_Qe^{-Q^2/4\lambda}+cg_Q^*e^{-Q^2/4\lambda})-\left(\frac{\lambda}{2}\right)^{1/2}\sum_W|f_W|^2\mathbf{W}_\parallel\cdot\mathbf{P}_0, \quad (18a)$$

$$E_n = {}_b\langle 0|_{b_{\mathbf{Q}}}\langle 0|\langle n|H_1|n\rangle|0\rangle_{b_{\mathbf{Q}}}|0\rangle_b$$
$$= \frac{\lambda}{2} + \frac{\beta^4}{32\lambda} + \frac{1}{4}P_0^2 + \sum_W \left(\omega_l + \frac{W_\parallel^2}{2}\right)(n + |f_W|^2) + \sum_Q \omega_s |g_Q|^2 + \sum_W \frac{1}{W}\sin(W_z z)(V_W^* f_W + V_W f_W^*)$$
$$+ \sum_Q \frac{1}{\sqrt{Q}} e^{-QZ}(c^* g_Q e^{-Q^2/4\lambda} + c g_Q^* e^{-Q^2/4\lambda}) - \left(\frac{\lambda}{2}\right)^{1/2} \sum_W (n + |f_W|^2)\mathbf{W}_\parallel \cdot \mathbf{P}_0, \tag{18b}$$

where $\mathbf{W}_\parallel$ is the wave vector in the x-y plane of the bulk LO phonon. The difference of the energy $E_n - E_0$ is

$$E_n - E_0 = \sum_W \left(\omega_l + \frac{W_\parallel^2}{2}\right) n - \left(\frac{\lambda}{2}\right)^{1/2} \sum_W n\mathbf{W}_\parallel \cdot \mathbf{P}_0. \tag{18c}$$

We are now going to calculate the perturbation energy due to the perturbing term H_2. Operating H_2 to $|0\rangle|0\rangle_{b_{\mathbf{Q}}}|0\rangle_b$, we have

$$H_2|0\rangle|0\rangle_{b_{\mathbf{Q}}}|0\rangle_b = \tfrac{1}{2}\sum_{W\neq W'} \mathbf{W}_\parallel \cdot \mathbf{W}'_\parallel f_W f_{W'} |1_{\mathbf{W}_\parallel}\rangle|1_{\mathbf{W}'_\parallel}\rangle, \tag{19a}$$

where

$$a_{\mathbf{W}}|0\rangle = 0, \quad a_{\mathbf{W}}^\dagger|0\rangle = |1_{\mathbf{W}_\parallel}\rangle, \quad a_{\mathbf{W}'}^\dagger|0\rangle = |1_{\mathbf{W}'_\parallel}\rangle,$$
$$\langle 0|0\rangle = 1, \quad \langle 1_{\mathbf{W}_\parallel}|1_{\mathbf{W}_\parallel}\rangle = 1, \quad \langle 1_{\mathbf{W}'_\parallel}|1_{\mathbf{W}'_\parallel}\rangle = 1, \tag{19b}$$

where $|1_{\mathbf{W}_\parallel}\rangle$ and $|1_{\mathbf{W}'_\parallel}\rangle$ are wave function of one phonon with wave vector $\mathbf{W}_\parallel$ and $\mathbf{W}'_\parallel$. In Eq. (19a), the summation is taken over all W and W' except $W = W'$. The diagonal elements of H_2 with respect to $|0\rangle|0\rangle_{b_{\mathbf{Q}}}|0\rangle_b$ vanish, as easily seen from Eq. (19a), and hence the first-order perturbation energy due to H_2 vanishes.[17] The matrix elements of the perturbed Hamiltonian H_2 is

$$(H_2)_{\text{no}} = {}_b\langle 0|_{b_{\mathbf{Q}}}\langle 0|\langle n|H_2|0\rangle|0\rangle_{b_{\mathbf{Q}}}|0\rangle_b$$
$$= \tfrac{1}{2}\sum_{W\neq W'} \mathbf{W}_\parallel \cdot \mathbf{W}'_\parallel f_W f_{W'} \quad \text{for } n = 1, \tag{20a}$$

$$(H_2)_{\text{no}} = {}_b\langle 0|_{b_{\mathbf{Q}}}\langle 0|\langle n|H_2|0\rangle|0\rangle_{b_{\mathbf{Q}}}|0\rangle_b = 0 \quad \text{for } n \neq 1. \tag{20b}$$

The energy correction in second order can be found from

$$\Delta E^{(2)} = -\sum_n{}' \frac{|(H_2)_{\text{no}}|^2}{E_n - E_0}. \tag{21a}$$

Substituting Eqs. (18c) and (20) into Eq. (21a), we have (see the Appendix)

$$\Delta E^{(2)} = -\alpha_l \omega_l, f_1(z) - \frac{\frac{1}{2}u^2}{\left[1 - \frac{\pi}{8}\alpha_l + 2\alpha_l L(z)\right]^2}$$
$$\times 2\alpha_l^2[3f_2(z) + f_3(z)], \tag{21b}$$

$$f_1(z) = \frac{1}{2}\int_0^\infty\int_0^\infty \frac{x^2y^2(1-e^{-2U_lZx})(1-e^{-2U_lZy})}{(1+x^2)^2(1+y^2)^2(2+x^2+y^2)}\,dx\,dy, \tag{21c}$$

$$f_2(z) = \int_0^\infty\int_0^\infty \frac{x^4y^2(1-e^{-2U_lZx})(1-e^{-2U_lZy})}{(1+x^2)^4(1+y^2)^2(2+x^2+y^2)}\,dx\,dy, \tag{21d}$$

$$f_3(z) = \int_0^\infty\int_0^\infty \frac{x^4y^2(1-e^{-2U_lZx})(1-e^{-2U_lZy})}{(1+x^2)^2(1+y^2)^2(2+x^2+y^2)^3}\,dx\,dy. \tag{21e}$$

In Eq. (21b), the first term being proportional to the squared coupling constant α_l^2 is extra energy of the induced potential of the surface magnetopolaron, which considers interaction between phonons of different wave vectors in the recoil process. The second term being proportional to the squared coupling constant α_l^2 is an extra effective mass of the surface magnetopolaron, which considers the corresponding interaction. Finally, the effective Hamiltonian of the surface magnetopolaron can be expressed as

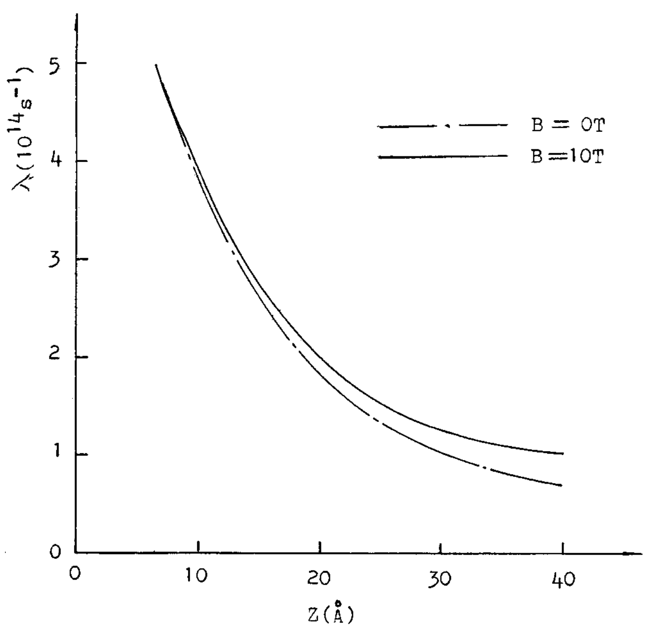

FIG. 1. The relation between the cyclotron-resonance frequency λ and the coordinate z in a AgCl crystal at different magnetic fields B.

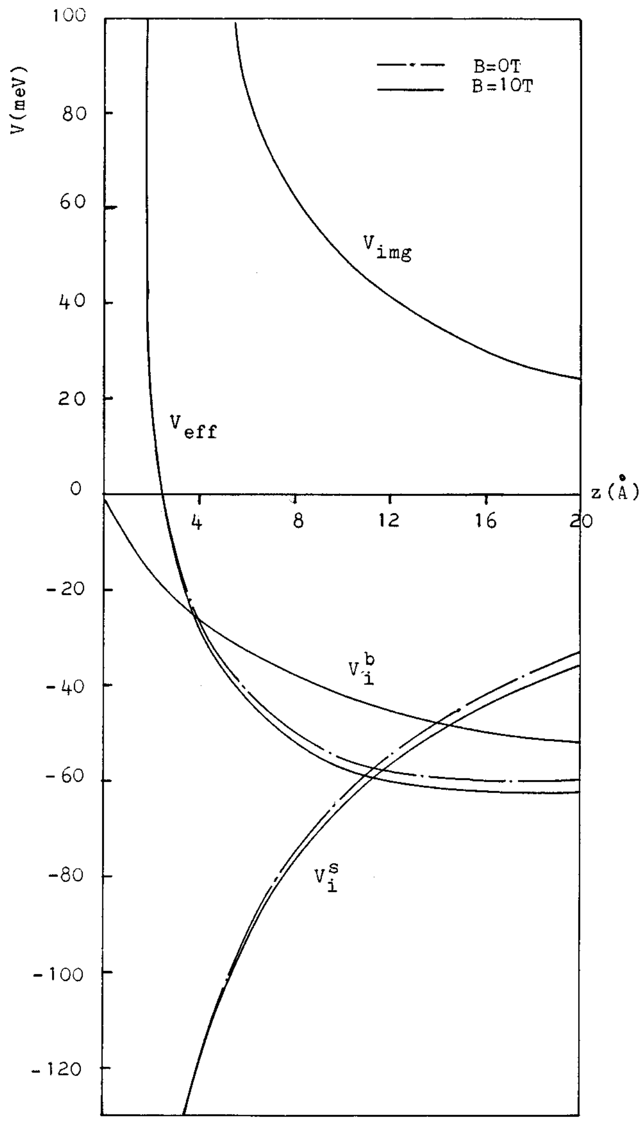

FIG. 2. The relation between the image potential V_{img}, the induced potential V_i^b, the induced potential V_i^s, and the effective interaction potential V_{eff} in a AgCl crystal with the coordinate z at different magnetic field B.

$$\mathcal{H}_{\mathrm{eff}}=H_z+\mathcal{H}_{\parallel\ \mathrm{eff}}+\Delta E^{(2)}=\frac{P_z^2}{2}+\frac{P_\parallel^2}{2m^*}+\frac{\lambda}{2}+\frac{\omega_c^2}{8\lambda}+V_{\mathrm{img}}+V_i^b+V_i^s, \tag{22a}$$

where

$$V_{\mathrm{img}}=\frac{e^2(\varepsilon_\infty-1)}{4z\varepsilon_\infty(\varepsilon_\infty+1)}, \tag{22b}$$

$$V_i^b=-\alpha_l\omega_l\left(\frac{\pi}{2}-K(z)\right)-\alpha_l^2\omega_l f_1(z), \tag{22c}$$

$$V_i^s=-\frac{\sqrt{\pi}}{2}\alpha_s\omega_s\left(\frac{\lambda}{\omega_s}\right)^{1/2}e^{-(\lambda/\omega_l)u_l^2z^2}\ \mathrm{erfc}\left[\left(\frac{\lambda}{\omega_l}\right)^{1/2}u_l z\right], \tag{22d}$$

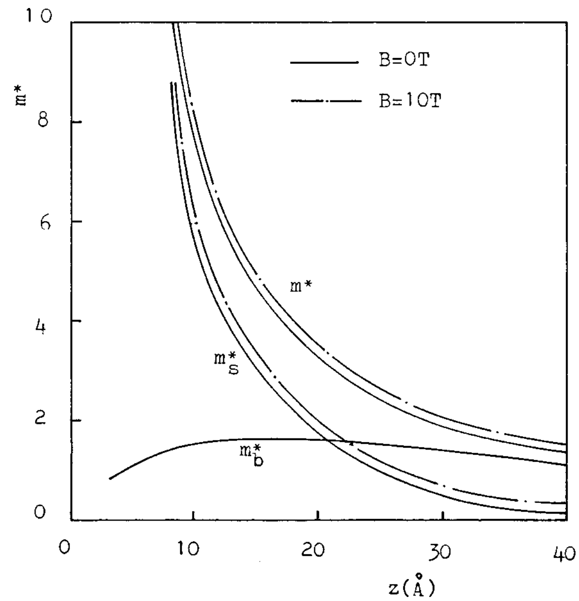

FIG. 3. The relation between the effective masses m^*, m_b^*, and m_s^* in a AgCl crystal with the coordinate z at different magnetic field B.

$$m^*=\left[\frac{1}{1-\frac{\pi}{8}\alpha_l+2\alpha_l L(z)}\left(1-\frac{2\alpha_l^2[3f_2(z)+f_3(z)]}{1-\frac{\pi}{8}\alpha_l+2\alpha_l L(z)}\right)+2\alpha_s\left(\frac{\lambda}{\omega_s}\right)^{3/2}M(z)\right] \tag{22e}$$

are the image potential, the potential induced by the electron-LO phonon interaction, the potential induced by the electron-SO phonon interaction, and the effective mass of the surface magnetopolaron, respectively. The effective interaction potential of the surface magnetopolaron is defined as

$$V_{\mathrm{eff}}=V_{\mathrm{img}}+V_i^b+V_i^s. \tag{22f}$$

Following Liang and Gu[23] we define the ''dead layer'' of the surface magnetopolaron. Its thickness is determined by

$$V_{\mathrm{eff}\ z=d}=0. \tag{23}$$

Evidently, the induced potential V_i^b, the effective mass m^*, and the thickness of the dead layer of the surface magnetopolaron depend on the interaction between phonons of different wave vectors in the recoil process.

IV. RESULTS AND DISCUSSION

In this section, taking the magnetopolaron in the surface of a AgCl crystal as an example, we perform a numerical

TABLE I. The data for a AgCl crystal. All the parameters are taken from Ref. 24.

Material	ε_0	ε_∞	$\hbar\omega_l$ (meV)	$\hbar\omega_s$ (meV)	α_l	α_S
AgCl	9.5	3.97	23.0	21.6	1.97	2.89

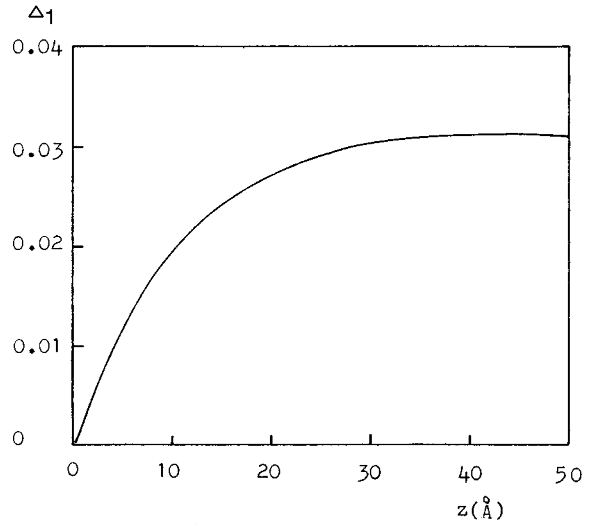

FIG. 4. The relation between Δ_1 with the coordinate z in a AgCl crystal.

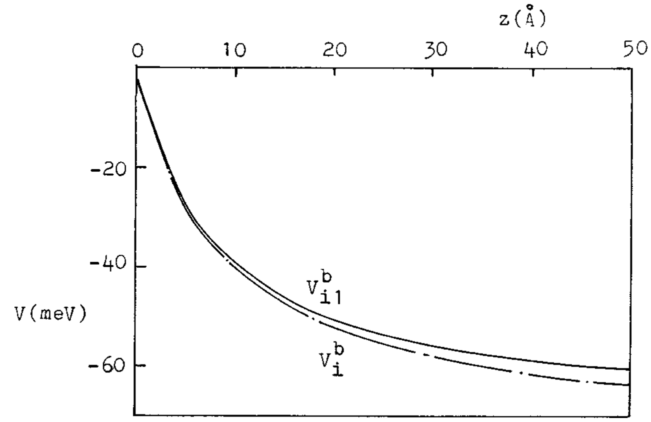

FIG. 6. The relation between V^b_{i1} and V^b_i with the coordinate z for a AgCl crystal.

evaluation. In Table I, the data for a AgCl crystal are given. Figure 1 shows the variation in the cyclotron-resonance frequency λ of the surface polaron in a AgCl crystal with the coordinate z at different magnetic fields B. The solid curve denotes the case $B=10$ T, and the broken curve represents the case $B=0$. From the figure, one can see that the cyclotron-resonance frequency λ will decrease with increasing z. At the same position (same value of z) the higher the magnetic field is, the higher the value of λ.

From Eqs. (22) and (23), one can see that there is only a magnetic field dependent on the electron-SO phonon interaction, the effective mass, the effective interaction potential, and the thickness of the dead layer of the surface polaron, whereas the image potential and the electron-bulk LO phonon interaction are independent of magnetic field. Figure 2 shows the relationship between the image potential V_{img}, the induced potential V^b_i resulting from the electron-bulk LO phonon interaction, the induced potential V^s_i resulting from the electron-SO phonon interaction, and the effective interaction potential V_{eff} of the surface magnetopolaron in AgCl crystal, which considers the interaction between phonons of different wave vectors in the recoil process, with the coordinate z at different magnetic fields B. The solid curve denotes the case $B=10$ T, and the broken curve represents the case $B=0$ T. From Fig. 2 one can see that the induced potential V^s_i of the surface magnetopolaron will decrease with increasing coordinate z, whereas the induced potential V^b_i will increase with increasing coordinate z. At the same position (same value of z), the higher the magnetic field, the higher the value of V^s_i. The effective interaction potential V_{eff} of the surface magnetopolaron in a AgCl crystal will decrease strongly with increasing the coordinate z for $z<d$ (thickness of the dead layer), whereas the absolute value of it increases with increasing the coordinate z for $z>d$. At the same position (same value of z), the higher the magnetic field B, the higher the absolute value of V_{eff}.

Near the surface, the electron-SO phonon interaction is

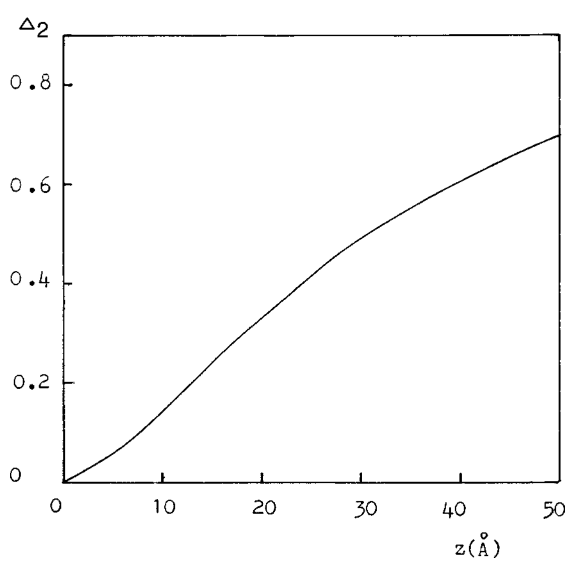

FIG. 5. The relation between Δ_2 with the coordinate z in a AgCl crystal.

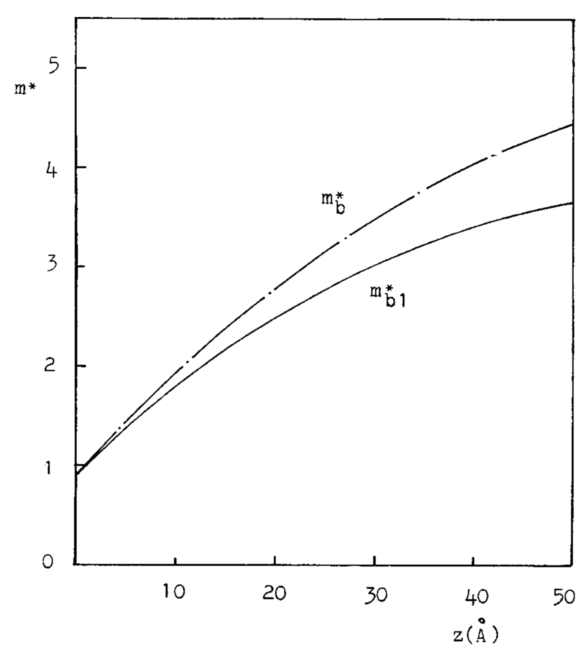

FIG. 7. The relation between m^*_{b1} and b^*_b with the coordinate z for a AgCl crystal.

dominant, whereas in the bulk far from the surface the electron-bulk–LO phonon interaction is dominant. From Eq. (22f), one can see that the surface magnetopolaron cannot get infinitely near the surface; there is no surface magnetopolaron in the range near the surface ($V_{\rm eff}>0$). Because of the similarity to the case of excitons we call the thin layer the surface magnetopolaron free-surface layer or dead layer of the surface magnetopolaron (for the AgCl crystal, $d=2.49$ Å). This shows that, when the distance between the electron and the surface is much smaller than the radius of the bulk polaron, the effect of the bulk phonons can be neglected and so can the effect of the surface phonons when the corresponding distance is much larger than the corresponding radius. In general, as the distance between the electron and the surface is the same order of magnitude as the radius of the bulk polaron, the effects of both the bulk LO and the SO phonons must be taken into account. In this case the electron moves in a nonlocal potential as Eq. (22a).

The effective mass m^* of the surface magnetopolaron can be expressed as

$$m^*=m_b^*+m_s^*, \tag{24a}$$

where

$$m_b^*=\frac{1}{1-\frac{\pi}{8}\alpha_l+2\alpha_l L(z)}\left(1-\frac{2\alpha_l^2[3f_2(z)+f_3(z)]}{1-\frac{\pi}{8}\alpha_l+2\alpha_l L(z)}\right), \tag{24b}$$

$$m_s^*=2\alpha_s\left(\frac{\lambda}{\omega_s}\right)^{3/2}M(z) \tag{24c}$$

are the effective mass induced by the electron-bulk LO phonon interaction and by the electron-SO phonon interaction, respectively. Figure 3 gives the relationship between the effective masses of the surface magnetopolaron m^*, m_b^*, and m_s^* in AgCl crystal, which considers the interaction between phonons of different wave vectors in the recoil process, with the coordinate z at different magnetic field B. The solid curve denotes the case $B=0$ T, and the broken curve represents the case $B=10$ T. From the figure one can see that effective mass m^* and the effective mass m_s^* induced by the electron-SO phonon interaction of the surface magnetopolaron will increase strongly with decreasing the coordinate z, whereas the effective mass m_b^* induced by the electron-bulk LO phonon interaction will increase little with increasing the coordinate z for $z<20$ Å, and it decreases little with increasing the coordinate z for $z>20$ Å. From the figure we also see that at the same position (same value of z), the higher the magnetic field B, the higher the value of m^* and m_s^*.

Since there is weak bulk but strong surface coupling between electrons and phonons in polar crystals, the interaction between phonons of different wave vectors in the recoil process influence only the induced potential V_i^b and the effective mass m_b^* resulting from the electron-bulk LO phonon interaction. The extra induced potential, which considers the interaction between phonons of different wave vectors in the recoil process, is given by

$$V_{l2}^b=-\alpha_l^2\omega_l f_1(z). \tag{25a}$$

The induced potential, which omits the corresponding interaction, is

$$V_{i1}^b=-\alpha_l\omega_l\left(\frac{\pi}{2}-K(Z)\right). \tag{25b}$$

The ratio of V_{i2}^b and V_{i1}^b is

$$\Delta_1=\frac{V_{i2}^b}{V_{i1}^b}=\alpha_l\,\frac{f_1(Z)}{\frac{\pi}{2}-K(Z)}. \tag{25c}$$

The extra effective mass, which considers the corresponding interaction, is given by

$$m_{b2}^*=\frac{2\alpha_l^2[3f_2(z)+f_3(z)]}{\left(1-\frac{\pi}{8}\alpha_l+2\alpha_l L(z)\right)^2}. \tag{26a}$$

The effective mass, which omits the corresponding interaction, is

$$m_{b1}^*=\frac{1}{1-\frac{\pi}{8}\alpha_l+2\alpha_l L(z)}. \tag{26b}$$

The ratio of m_{b2}^* and m_{b1}^* is

$$\Delta_2=\frac{m_{b2}^*}{m_{b1}^*}=\frac{2\alpha_l^2[3f_2(z)+f_3(z)]}{1-\frac{\pi}{8}\alpha_l+2\alpha_l L(z)}. \tag{26c}$$

Figures 4 and 5 gives a description of the variation of Δ_1 and Δ_2 with the coordinate z in a AgCl crystal. From Figs. 4 and 5 one can see that Δ_1 and Δ_2 will increase with increasing the coordinate z.

Figure 6 shows the relationship between the induced potential V_{i1}^b, which omits the corresponding interaction, and the induced potential V_i^b of the surface magnetopolaron in a AgCl crystal, which considers the corresponding interaction, with the coordinate z. The solid curve denotes the case of V_{i1}^b and the dashed one represents the case of V_i^b. From the figure, we can see that the induced potential V_{i1}^b and V_i^b will increase with increasing the coordinate z; moreover, V_i^b will increase more than V_{i1}^b with increasing the coordinate z. Figure 7 shows the variation of the effective mass m_b^*, which considers the corresponding interaction, and the effective mass m_{b1}^*, which omits the corresponding interaction, with the coordinate z. The solid curve denotes the case of m_{b1}^*; the dashed one represents the case of m_b^*. It can be seen from Fig. 7 that the effective masses m_{b1}^* and m_b^* will increase with increasing the coordinate z; moreover, m_b^* will increase more than m_{b1}^* with increasing the coordinate z.

ACKNOWLEDGMENT

One of us (J. L. Xiao) wishes to acknowledge support by the National Science Foundation of Inner Mongolia.

APPENDIX

To calculate the second-order perturbation correction $\Delta E^{(2)}$, substituting Eqs. (18c) and (20) into Eq. (21a), we have

$$\Delta E^{(2)}=-\sum_{W\neq W'}\frac{\frac{1}{4}(\mathbf{W}_\parallel\cdot\mathbf{W}'_\parallel)^2|V_W|^2|V_{W'}|^2\ \sin^2(W_zZ)\sin^2(W'_zZ)}{\left[2\omega_l+\frac{1}{2}(W_\parallel^2+W_\parallel'^2)-\left(\frac{\lambda}{2}\right)^{1/2}(\mathbf{W}_\parallel+\mathbf{W}'_\parallel)\cdot\mathbf{P}_0\right]}$$
$$\times\frac{1}{W^2\left[\omega_l+\frac{1}{2}W_\parallel^2-\left(\frac{\lambda}{2}\right)^{1/2}\mathbf{W}_\parallel\cdot\mathbf{P}_0\right]^2W'^2\left[\omega_l+\frac{1}{2}\ W_\parallel'^2-\left(\frac{\lambda}{2}\right)^{1/2}\mathbf{W}'_\parallel\cdot\mathbf{P}_0\right]^2}. \tag{A1}$$

Equation (A1) can be represented as

$$\Delta E^{(2)}=-\sum_{W\neq W'}\frac{\frac{1}{4}(\mathbf{W}_\parallel\cdot\mathbf{W}'_\parallel)^2|V_W|^2|V_{W'}|^2\ \sin^2(W_zZ)\sin^2(W'_zZ)}{[2\omega_l+\frac{1}{2}(W_\parallel^2+W_\parallel'^2)]W^2(\omega_l+\frac{1}{2}W_\parallel^2)^2W'^2(\omega_l+\frac{1}{2}W_\parallel'^2)^2}$$
$$\times\left(1+\frac{\left(\frac{\lambda}{2}\right)^{1/2}(\mathbf{W}_\parallel+\mathbf{W}'_\parallel)\cdot\mathbf{P}_0}{2\omega_l+\frac{1}{2}(W_\parallel^2+W_\parallel'^2)}+\frac{\frac{\lambda}{2}[(\mathbf{W}_\parallel+\mathbf{W}'_\parallel)\cdot\mathbf{P}_0]^2}{[2\omega_l+\frac{1}{2}(W_\parallel^2+W_\parallel'^2)]^2}+\cdots\right)\left(1+\frac{2\left(\frac{\lambda}{2}\right)^{1/2}\mathbf{W}_\parallel\cdot\mathbf{P}_0}{\omega_l+\frac{1}{2}W_\parallel^2}+\frac{3\frac{\lambda}{2}(\mathbf{W}_\parallel\cdot\mathbf{P}_0)^2}{(\omega_l+\frac{1}{2}W_\parallel^2)^2}+\cdots\right)$$
$$\times\left(1+\frac{2\left(\frac{\lambda}{2}\right)^{1/2}\mathbf{W}'_\parallel\cdot\mathbf{P}_0}{\omega_l+\frac{1}{2}W_\parallel'^2}+\frac{3\frac{\lambda}{2}(\mathbf{W}'_\parallel\cdot\mathbf{P}_0)^2}{(\omega_l+\frac{1}{2}W_\parallel'^2)^2}+\cdots\right). \tag{A2}$$

Equation (A2) can be calculated by replacing the summation with integration and expanding them up to the second-order term of $\mathbf{W}_\parallel\cdot\mathbf{P}_0$ and $\mathbf{W}'_\parallel\cdot\mathbf{P}_0$ for a slow electron.[18] In this expression, the first-order terms in $\mathbf{W}_\parallel\cdot\mathbf{P}_0$ and $\mathbf{W}'_\parallel\cdot\mathbf{P}_0$ are equal to zero. In calculating Eq. (A2), it is convenient to choose the x axis parallel to the $\mathbf{P}_0$ direction and the x-y plane coincident with the plane determined by $\mathbf{P}_0$, $\mathbf{W}_\parallel$, and $\mathbf{W}'_\parallel$; thus the relative vectors may be expressed as

$$\mathbf{P}_0=P_0(1,0),$$
$$\mathbf{W}_\parallel=\mathbf{W}_\parallel(\cos\ \varphi,\sin\ \varphi),$$
$$\mathbf{W}'_\parallel=W'_\parallel(\cos\ \varphi',\sin\ \varphi'). \tag{A3}$$

W (W'), W_z (W'_z), and $W_\parallel$ $(W'_\parallel)$ satisfy

$$W^2=W_z^2+W_\parallel^2,\quad W'^2=W_z'^2+W_\parallel'^2. \tag{A4}$$

Thus, $\Delta E^{(2)}$ can be expressed as

$$\Delta E^{(2)}=\Delta E_1^{(2)}+\Delta E_2^{(2)}+\Delta E_3^{(2)}+\Delta E_4^{(2)}, \tag{A5}$$

where

$$\Delta E_1^{(2)}=-\frac{1}{4}\left(\frac{S}{4\pi^2}\right)^2\left(\frac{L}{2\pi}\right)^2\int_0^{2\pi}d\varphi\int_0^{2\pi}d\varphi'\int_0^\infty dW_z\int_0^\infty dW'_z\int_0^\infty dW_\parallel\int_0^\infty dW'_\parallel$$
$$\times\frac{W_\parallel^2W_\parallel'^2|V_W|^2|V_{W'}|^2\sin^2(W_zz)\sin^2(W'_zz)(\cos^2\varphi\ \cos^2\varphi'+\sin^2\varphi\ \sin^2\varphi')}{[2\omega_l+\frac{1}{2}(W_\parallel^2+W_\parallel'^2)](W_z^2+W_\parallel^2)(\omega_l+\frac{1}{2}W_\parallel^2)^2(W_z'^2+W_\parallel'^2)(\omega_l+\frac{1}{2}W_\parallel'^2)^2}$$
$$=-\alpha_l^2\omega_lf_1(z), \tag{A6}$$

$$\Delta E_2^{(2)}=\Delta E_3^{(2)}=-\frac{1}{4}\left(\frac{S}{4\pi^2}\right)^2\left(\frac{L}{2\pi}\right)^2\int_0^{2\pi}d\varphi\int_0^{2\pi}d\varphi'\int_0^{\infty}dW_Z\int_0^{\infty}dW'_Z\int_0^{\infty}dW_\parallel\int_0^{\infty}dW'_\parallel$$
$$\times\frac{\frac{3}{2}\lambda P_0^2W_\parallel^4W_\parallel'^2|V_W|^2|V_{W'}|^2\sin^2(W_zz)\sin^2(W'_zz)(\cos^2\varphi\ \cos^2\varphi'+\sin^2\varphi\ \sin^2\varphi')\cos^2\varphi}{[2\omega_l+\frac{1}{2}(W_\parallel^2+W_\parallel'^2)](W_z^2+W_\parallel^2)(\omega_l+\frac{1}{2}W_\parallel^2)^4(W_z'^2+W_\parallel'^2)(\omega_l+\frac{1}{2}W_\parallel'^2)^2}$$
$$=-\frac{u^2}{2}\frac{3\alpha_l^2}{\left(1-\frac{\pi}{8}\alpha_l+2\alpha_lL(z)\right)^2}f_2(z), \tag{A7}$$

$$\Delta E_4^{(2)}=-\frac{1}{4}\left(\frac{S}{4\pi^2}\right)^2\left(\frac{L}{2\pi}\right)^2\int_0^{2\pi}d\varphi\int_0^{2\pi}d\varphi'\int_0^{\infty}dW_z\int_0^{\infty}dW'_z\int_0^{\infty}dW_\parallel\int_0^{\infty}dW'_\parallel$$
$$\times\frac{\frac{\lambda}{2}P_0^2W_\parallel^2W_\parallel'^2|V_W|^2|V_{W'}|^2\sin^2(W_zz)\sin^2(W'_zz)(W_\parallel^2\cos^2\varphi+W_\parallel'^2\cos^2\varphi')(\cos^2\varphi\ \cos^2\varphi'+\sin^2\varphi\ \sin^2\varphi')}{[2\omega_l+\frac{1}{2}(W_\parallel^2+W_\parallel'^2)]^3(W_z^2+W_\parallel^2)(\omega_l+\frac{1}{2}W_\parallel^2)^2(W_z'^2+W_\parallel'^2)(\omega_l+\frac{1}{2}W_\parallel'^2)^2}$$
$$=-\frac{u^2}{2}\frac{2\alpha_l^2}{\left(1-\frac{\pi}{8}\alpha_l+2\alpha_lL(z)\right)^2}f_3(z). \tag{A8}$$

Finally, we can obtain the second-order perturbation correction $\Delta E^{(2)}$.

---

*Mailing address.

[1] K. K. Bajaj, Phys. Rev. **170**, 694 (1968); Nuovo Cimento B **55**, 244 (1968).
[2] Y. Lepine and D. Watz, Can. J. Phys. **54**, 1979 (1976).
[3] S. Das Sarma, Phys. Rev. Lett. **52**, 859 (1984).
[4] F. M. Peeters and J. T. Devreese, Phys. Rev. B **33**, 4338 (1986).
[5] E. Evans and L. Mills, Solid State Commun. **11**, 1093 (1972).
[6] E. Evans and L. Mills, Phys. Rev. B **8**, 4004 (1973).
[7] D. M. Larsen, Phys. Rev. B **33**, 799 (1986).
[8] X. J. Kong, C. W. Wei, and S. W. Gu, Phys. Rev. B **39**, 3230 (1989).
[9] F. A. P. Osorio, M. Z. Maialle, and O. Hipolito, Solid State Commun. **80**, 567 (1991).
[10] Ze. Hu *et al.*, J. Phys.: Condens. Matter **4**, 5089 (1992).
[11] B. H. Wei, K. W. Yu, and F. Ou, J. Phys.: Condens. Matter **6**, 1893 (1994).
[12] B. H. Wei and K. W. Yu, J. Phys.: Condens. Matter **7**, 1959 (1995).
[13] J. Huybrechts, J. Phys. C **9**, L211 (1976).
[14] N. Tokuda, J. Phys. C **13**, L173 (1980).
[15] S. W. Gu and J. Zheng, Phys. Status Solidi B **121**, K165 (1984).
[16] N. Tokuda, J. Phys. C **13**, L851 (1980).
[17] E. Haga, Prog. Theor. Phys. **11**, 449 (1954).
[18] J. S. Pan, Phys. Status Solidi B **127**, 307 (1985).
[19] B. Q. Sun, W. Xiao, and J. L. Xiao, J. Phys.: Condens. Matter **6**, 8167 (1994).
[20] J. L. Xiao, B. Q. Sun, and W. Xiao, Phys. Status Solidi B **176**, 117 (1993).
[21] J. L. Xiao, T. H. Xing, B. Q. Sun, and W. Xiao, Phys. Status Solidi B **183**, 425 (1994).
[22] B. H. Wei, Y. Y. Liu, S. W. Gu, and W. K. Yu, Phys. Rev. B **46**, 4269 (1992).
[23] X. X. Liang and S. W. Gu, Solid State Commun. **50**, 505 (1984).
[24] E. Kartheuser, *Polarons in Ionic Crystals and Polar Semiconductors* (North-Holland, Amsterdam, 1972).